Proceedings of the ASME 2014 International Design Engineering Technical Conferences & Computers and Information in Engineering Conference
IDETC/CIE 2014
August 17-20, 2014, Buffalo, NY, USA

DETC2014-35349

BI-LINEAR SHEAR DEFORMABLE ANCF SHELL ELEMENT USING CONTINUUM MECHANICS APPROACH

Hiroki Yamashita
Department of Mechanical and Industrial Engineering
The University of Iowa
Iowa City, Iowa 52242

Antti I. Valkeapää
Department of Mechanical Engineering
Lappeenranta University of Technology
Skinnarilankatu 34,
53850 Lappeenranta, Finland

Paramsothy Jayakumar
US Army RDECOM TARDEC
6501 E. 11 Mile Road
Warren, MI 48397-5000

Hiroyuki Sugiyama
Department of Mechanical and Industrial Engineering
The University of Iowa
Iowa City, Iowa 52242

ABSTRACT

In this investigation, a bi-linear shear deformable shell element is developed using the absolute nodal coordinate formulation for the large deformation analysis of multibody shell structures. The element consists of four nodes, each of which has the global position coordinates and the gradient coordinates along the thickness introduced for describing the orientation and deformation of the cross section of the shell element. The global position field on the mid-plane and the position vector gradient at a material point in the element are interpolated by bi-linear polynomials. The continuum mechanics approach is used to formulate the generalized elastic forces, allowing for the consideration of nonlinear constitutive models in a straightforward manner. The element locking exhibited in this type of element can be eliminated using the assumed natural strain (ANS) and enhanced assumed strain (EAS) approaches. In particular, the combined ANS and EAS approach is introduced to alleviate the thickness locking arising from the erroneous transverse normal strain distribution. Several numerical examples are presented in order to demonstrate the accuracy and the rate of convergence of numerical solutions obtained by the bi-linear shear deformable ANCF shell element proposed in this investigation.

1. INTRODUCTION

The plate elements of the absolute nodal coordinate formulation (ANCF) can be classified into the fully parameterized shear deformable element [1] and the gradient deficient thin plate element [2]. While the fully parameterized element leads to a general motion description that accounts for coupled deformation modes including complex cross-section deformation modes of the plate and shell elements, use of higher order polynomials and the coupled deformation modes exhibited in this type of element cause severe element locking that needs to be carefully treated [3,4]. The gradient deficient plate elements, on the other hand, can be developed by eliminating the position vector gradient coordinate along the thickness ($\partial \mathbf{r} / \partial z$), thus the global displacement field on the mid-plane can be uniquely parameterized by the global position vector and the two gradient vectors $\partial \mathbf{r} / \partial x$ and $\partial \mathbf{r} / \partial y$ which are both tangent to the surface. By doing so, the cross-section is assumed to be rigid and the elastic forces are derived using an in-plane stress assumption with Kirchhoff-Love plate theory in a straightforward manner. While the element does not suffer from severe element locking problems, the element can be applied to problems of thin plate and shell structures only.

In recent years, the ANCF parameterization, which eliminates the position vector gradients tangent to the surface, are investigated. The position vector gradient along the plate thickness is used to describe the orientation and deformation of the cross-section, allowing for describing the shear and thickness deformation of the plate. The two- and three-dimensional beam elements that eliminate the gradient vector

Report Documentation Page

Form Approved
OMB No. 0704-0188

1. REPORT DATE	2. REPORT TYPE	3. DATES COVERED
24 FEB 2014	**Journal Article**	**18-03-2013 to 27-01-2014**

4. TITLE AND SUBTITLE
BI-LINEAR SHEAR DEFORMABLE ANCF SHELL ELEMENT USING CONTINUUM MECHANICS APPROACH

5a. CONTRACT NUMBER
W56HZV-04-2-0001

5b. GRANT NUMBER

5c. PROGRAM ELEMENT NUMBER

6. AUTHOR(S)
Hiroki Yamashita; Antti Valkeapaa; Paramsothy Jayakumar; Hiroyuki Sugiyama

5d. PROJECT NUMBER

5e. TASK NUMBER

5f. WORK UNIT NUMBER

7. PERFORMING ORGANIZATION NAME(S) AND ADDRESS(ES)
Department of Mechanical and Industrial Engineering,The University of Iowa,101 Jessup Hall,Iowa City,IA,55242

8. PERFORMING ORGANIZATION REPORT NUMBER
; #24404

9. SPONSORING/MONITORING AGENCY NAME(S) AND ADDRESS(ES)
U.S. Army TARDEC, 6501 East Eleven Mile Rd, Warren, Mi, 48397-5000

10. SPONSOR/MONITOR’S ACRONYM(S)
TARDEC

11. SPONSOR/MONITOR’S REPORT NUMBER(S)
#24404

12. DISTRIBUTION/AVAILABILITY STATEMENT
Approved for public release; distribution unlimited

13. SUPPLEMENTARY NOTES
Proceedings of the ASME 2014 International Design Engineering Technical Conferences & Computers and Information in Engineering Conference IDETC/CIE 2014

14. ABSTRACT
In this investigation, a bi-linear shear deformable shell element is developed using the absolute nodal coordinate formulation for the large deformation analysis of multibody shell structures. The element consists of four nodes, each of which has the global position coordinates and the gradient coordinates along the thickness introduced for describing the orientation and deformation of the cross section of the shell element. The global position field on the mid-plane and the position vector gradient at a material point in the element are interpolated by bi-linear polynomials. The continuum mechanics approach is used to formulate the generalized elastic forces, allowing for the consideration of nonlinear constitutive models in a straightforward manner. The element locking exhibited in this type of element can be eliminated using the assumed natural strain (ANS) and enhanced assumed strain (EAS) approaches. In particular, the combined ANS and EAS approach is introduced to alleviate the thickness locking arising from the erroneous transverse normal strain distribution. Several numerical examples are presented in order to demonstrate the accuracy and the rate of convergence of numerical solutions obtained by the bi-linear shear deformable ANCF shell element proposed in this investigation.

15. SUBJECT TERMS

16. SECURITY CLASSIFICATION OF:			17. LIMITATION OF ABSTRACT	18. NUMBER OF PAGES	19a. NAME OF RESPONSIBLE PERSON
a. REPORT **unclassified**	b. ABSTRACT **unclassified**	c. THIS PAGE **unclassified**	**Public Release**	**8**	

Standard Form 298 (Rev. 8-98)
Prescribed by ANSI Std Z39-18

along the beam centerline are proposed in the literatures [6], while a bi-linear shear deformable ANCF plate element is discussed in the literature [5], in which a selective reduced integration is used for eliminating the transverse shear locking. The use of such an element parameterization allows for developing shear deformable plate elements while reducing the number of coordinates per node. Furthermore, it is shown in the literature [7] that the element locking problems exhibited in the bi-linear shear deformable ANCF plate element based on the elastic plane approach can be alleviated by the assumed natural strain (ANS) approach for the transverse shear and the transverse normal (thickness) strains, while the enhanced assumed strain (EAS) approach is applied to the in-plane normal and shear locking. Since the elastic forces are formulated using an elastic plane approach, in which the strain distribution along the thickness is assumed to be constant, the element can be applied to moderately thick and flat plate problems and, at the same time, consideration of nonlinear material models requires specialized formulations. It is, therefore, the objective of this investigation to generalize the bi-linear shear deformable ANCF plate element based on the elastic plane approach to the shell element using continuum mechanics approach, which allows for the consideration of nonlinear constitutive models in a straightforward manner.

2. KINEMATICS OF BI-LINEAR SHEAR DEFORMABLE ANCF ELEMENT

As shown in Fig. 1, the global position vector $\mathbf{r}^i$ of a material point $\mathbf{x}^i = [x^i \quad y^i \quad z^i]^{\mathrm{T}}$ in a shell element i is defined as

$$\mathbf{r}^i = \mathbf{r}_m^i(x^i, y^i) + z^i \frac{\partial \mathbf{r}_m^i}{\partial z^i}(x^i, y^i) \tag{1}$$

where $\mathbf{r}_m^i(x^i, y^i)$ is the global position vector on the mid-plane and $\partial \mathbf{r}_m^i(x^i, y^i) / \partial z^i$ is the transverse gradient vector used to describe the orientation and deformation of the infinitesimal volume in the element. The preceding global displacement field is interpolated using the bi-linear polynomials as follows:

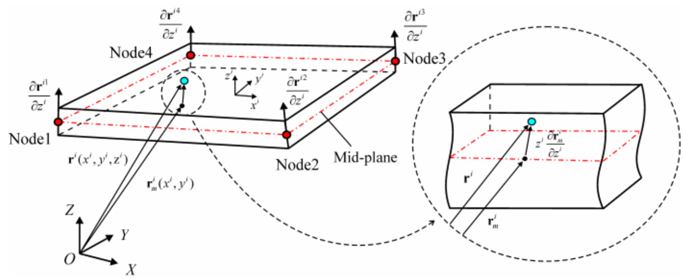

Figure 1. Kinematics of bi-linear ANCF element

$$r^i = a_0 + a_1 x^i + a_2 y^i + a_3 x^i y^i + z^i (a_4 + a_5 x^i + a_6 y^i + a_7 x^i y^i) \tag{2}$$

from which, one can interpolate both displacement field on the mid-plane and the transverse gradient vector as

$$\mathbf{r}_m^i(x^i, y^i) = \mathbf{S}_m^i(x^i, y^i)\mathbf{e}_m^i, \quad \frac{\partial \mathbf{r}_m^i}{\partial z^i}(x^i, y^i) = \mathbf{S}_m^i(x^i, y^i)\mathbf{e}_g^i \tag{3}$$

where $\mathbf{S}_m^i = \left[S_1^i\mathbf{I} \quad S_2^i\mathbf{I} \quad S_3^i\mathbf{I} \quad S_4^i\mathbf{I} \right]$ is the bi-linear shape function matrix and

$$\begin{aligned} S_1^i &= \frac{1}{4}(1-\xi^i)(1-\eta^i), \quad S_2^i = \frac{1}{4}(1+\xi^i)(1-\eta^i), \\ S_3^i &= \frac{1}{4}(1+\xi^i)(1+\eta^i), \quad S_4^i = \frac{1}{4}(1-\xi^i)(1+\eta^i) \end{aligned} \tag{4}$$

where $\xi^i = x^i / \ell^i$ and $\eta^i = y^i / w^i$. ℓ^i and w^i are lengths along the element x^i and y^i axes, respectively. In Eq. 3, the vectors $\mathbf{e}_m^i$ and $\mathbf{e}_g^i$ represent the element nodal coordinates associated with the global position vector on the mid-plane and the transverse gradient vector. That is, for node k of element i, one has $\mathbf{e}_m^{ik} = \mathbf{r}^{ik}$ and $\mathbf{e}_g^{ik} = \partial \mathbf{r}^{ik} / \partial z^i$. It is important to notice here that the assumed displacement field $\mathbf{r}_m^i$ on the mid-plane does not involve any gradient coordinates, while the orientation and deformation of the infinitesimal volume at the material point in the shell element is parameterized by the transverse gradient coordinates. Substitution of Eq. 3 into Eq. 1 leads to the following general expression for the global position vector used for the absolute nodal coordinate formulation:

$$\mathbf{r}^i(x^i, y^i, z^i) = \mathbf{S}^i(x^i, y^i, z^i)\mathbf{e}^i \tag{5}$$

where the shape function matrix $\mathbf{S}^i$ and the element nodal coordinates are, respectively, defined as

$$\mathbf{S}^i = \left[\mathbf{S}_m^i \quad z^i\mathbf{S}_m^i \right], \quad \mathbf{e}^i = [(\mathbf{e}_m^i)^T \quad (\mathbf{e}_g^i)^T]^T \tag{6}$$

3. BI-LINEAR SHEAR DEFORMABLE ANCF SHELL ELEMENT

3.1 Generalized Elastic Forces using Continuum Mechanics Approach

The Green-Lagrange strain tensor $\mathbf{E}^i$ of element *i* is defined as

$$\mathbf{E}^i = \frac{1}{2}\left((\mathbf{F}^i)^T \mathbf{F}^i - \mathbf{I}\right) \tag{7}$$

where the displacement gradient tensor $\mathbf{F}^i$ is defined by

$$\mathbf{F}^i = \frac{\partial \mathbf{r}^i}{\partial \mathbf{X}^i} = \frac{\partial \mathbf{r}^i}{\partial \mathbf{x}^i}\left(\frac{\partial \mathbf{X}^i}{\partial \mathbf{x}^i}\right)^{-1} = \bar{\mathbf{J}}^i\,(\mathbf{J}^i)^{-1} \tag{8}$$

In the preceding equation, $\bar{\mathbf{J}}^i = \partial \mathbf{r}^i / \partial \mathbf{x}^i$ and $\mathbf{J}^i = \partial \mathbf{X}^i / \partial \mathbf{x}^i$, where the vector $\mathbf{X}^i$ represents the global position vector of element *i* at the reference configuration. Substitution of Eq. 8 into Eq. 7 leads to

$$\mathbf{E}^i = (\mathbf{J}^i)^{-T}\,\tilde{\mathbf{E}}^i\,(\mathbf{J}^i)^{-1} \tag{9}$$

where $\tilde{\mathbf{E}}^i$ is the covariant strain tensor defined by

$$\tilde{\mathbf{E}}^i = \frac{1}{2}\left((\bar{\mathbf{J}}^i)^T \bar{\mathbf{J}}^i - (\mathbf{J}^i)^T \mathbf{J}^i\right) \tag{10}$$

The transformation (push-forward operation) of the covariant strain tensor $\tilde{\mathbf{E}}^i$ given by Eq. 9 can be re-expressed in a form of the vector transformation by introducing the engineering covariant strain vector $\tilde{\boldsymbol{\varepsilon}}^i$ as

$$\boldsymbol{\varepsilon}^i = (\mathbf{T}^i)^{-T}\,\tilde{\boldsymbol{\varepsilon}}^i \tag{11}$$

where

$$\tilde{\boldsymbol{\varepsilon}}^i = [\tilde{\varepsilon}^i_{xx} \quad \tilde{\varepsilon}^i_{yy} \quad \tilde{\gamma}^i_{xy} \quad \tilde{\varepsilon}^i_{zz} \quad \tilde{\gamma}^i_{xz} \quad \tilde{\gamma}^i_{yz}]^T \tag{12}$$

and the vector $\boldsymbol{\varepsilon}$ indicates the engineering strain vector associated with Green-Lagrange strain tensor given by Eq. 7. The transformation matrix $\mathbf{T}^i$ in Eq. 11 can be expressed explicitly as

$$\mathbf{T}^i = \begin{bmatrix} (J^i_{11})^2 & (J^i_{12})^2 & 2J^i_{11}J^i_{12} & (J^i_{13})^2 & 2J^i_{11}J^i_{13} & 2J^i_{12}J^i_{13} \\ (J^i_{21})^2 & (J^i_{22})^2 & 2J^i_{21}J^i_{22} & (J^i_{23})^2 & 2J^i_{21}J^i_{23} & 2J^i_{22}J^i_{23} \\ J^i_{11}J^i_{21} & J^i_{12}J^i_{22} & J^i_{11}J^i_{22}+J^i_{12}J^i_{21} & J^i_{13}J^i_{23} & J^i_{11}J^i_{23}+J^i_{13}J^i_{21} & J^i_{12}J^i_{23}+J^i_{13}J^i_{22} \\ (J^i_{31})^2 & (J^i_{32})^2 & 2J^i_{31}J^i_{32} & (J^i_{33})^2 & 2J^i_{31}J^i_{33} & 2J^i_{32}J^i_{33} \\ J^i_{11}J^i_{31} & J^i_{12}J^i_{32} & J^i_{11}J^i_{32}+J^i_{12}J^i_{31} & J^i_{13}J^i_{33} & J^i_{11}J^i_{33}+J^i_{13}J^i_{31} & J^i_{12}J^i_{33}+J^i_{13}J^i_{32} \\ J^i_{21}J^i_{31} & J^i_{22}J^i_{32} & J^i_{21}J^i_{32}+J^i_{22}J^i_{31} & J^i_{23}J^i_{33} & J^i_{21}J^i_{33}+J^i_{23}J^i_{31} & J^i_{22}J^i_{33}+J^i_{23}J^i_{32} \end{bmatrix} \tag{13}$$

and J^i_{ab} is the element in the *a*-th column and *b*-th row of matrix $\mathbf{J}^i$. The generalized elastic forces can then be obtained using the virtual work as

$$\mathbf{Q}^i_k = \int_{V^i_0} \left(\frac{\partial \boldsymbol{\varepsilon}^i}{\partial \mathbf{e}^i}\right)^T \boldsymbol{\sigma}^i\, dV^i_0 \tag{14}$$

where $\boldsymbol{\sigma}^i$ is a vector of the second Piola–Kirchhoff stresses and dV^i_0 is the infinitesimal volume at the reference configuration of element *i*. It is important to notice here that the element elastic forces are evaluated as a continuum volume, and a wide variety of nonlinear constitutive models such as hyperelasticity for large deformation problems can be considered in the shell element in a straight forward manner.

3.2 Element Locking for Transverse Shear and In-Plane Strains

As it has been addressed in many literatures of shell element formulations [8-17], the bi-linear quadrilateral shell element suffers mainly from the element locking associated with the transverse shear and the in-plane strain components. It is well known that the transverse shear locking can be elegantly eliminated using the assumed natural strain (ANS) approach proposed by Bathe and Dvorkin [10,11]. In this approach, the covariant shear strain components are interpolated using those evaluated at the sampling points *A*, *B*, *C* and *D* shown in Fig. 2 as follows:

$$\left.\begin{aligned} \tilde{\gamma}^{ANS}_{xz} &= \frac{1}{2}(1-\eta)\,\tilde{\gamma}^{C}_{xz} + \frac{1}{2}(1+\eta)\,\tilde{\gamma}^{D}_{xz} \\ \tilde{\gamma}^{ANS}_{yz} &= \frac{1}{2}(1-\xi)\,\tilde{\gamma}^{A}_{yz} + \frac{1}{2}(1+\xi)\,\tilde{\gamma}^{B}_{yz} \end{aligned}\right\} \tag{15}$$

where $\tilde{\gamma}^A_{yz}$, $\tilde{\gamma}^B_{yz}$, $\tilde{\gamma}^C_{xz}$ and $\tilde{\gamma}^D_{xz}$ are the compatible strains at the sampling points.

The parasitic in-plane shear under pure bending loads is a typical locking problem exhibited in the bi-linear quadrilateral element [18], and the compatible in-plane strain vector obtained by the assumed displacement field can be enhanced by introducing the enhanced assumed strain (EAS) $\boldsymbol{\varepsilon}^{EAS}$ as [8]

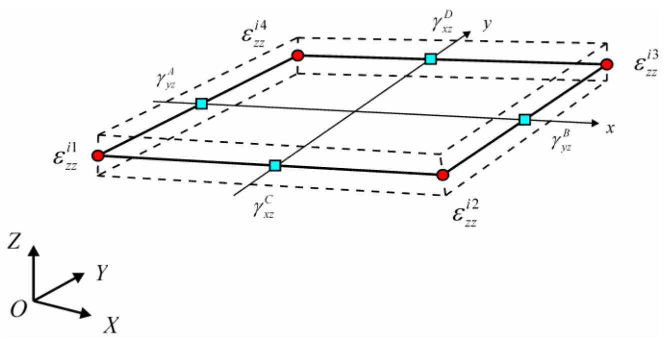

Figure 2. Sampling points for assumed natural strain

$$\boldsymbol{\varepsilon} = \boldsymbol{\varepsilon}^c + \boldsymbol{\varepsilon}^{EAS} \tag{16}$$

and $\boldsymbol{\varepsilon}^{EAS}$ is defined by

$$\boldsymbol{\varepsilon}^{EAS}(\boldsymbol{\xi}) = \mathbf{G}(\boldsymbol{\xi})\boldsymbol{\alpha} \tag{17}$$

where $\boldsymbol{\alpha}$ is a vector of internal parameters introduced to define the enhanced strain field and the matrix $\mathbf{G}(\boldsymbol{\xi})$ is given as [8]

$$\mathbf{G}(\boldsymbol{\xi}) = \frac{|\mathbf{J}_0|}{|\mathbf{J}(\boldsymbol{\xi})|}\mathbf{T}_0^{-\mathrm{T}}\mathbf{M}(\boldsymbol{\xi}) \tag{18}$$

where $\mathbf{J}(\boldsymbol{\xi})$ and $\mathbf{J}_0$ are defined as a position vector gradient at the reference configuration evaluated at the integration point $\boldsymbol{\xi}$ and at the center of element ($\boldsymbol{\xi} = \mathbf{0}$), respectively. $\boldsymbol{\xi}$ is a vector of the element coordinates in the parametric domain and $\mathbf{T}_0$ is the transformation matrix evaluated at the center of element [8,9]. The matrix $\mathbf{M}(\boldsymbol{\xi})$ defines polynomials introduced to enhance the strain field. Using Eq. 18, the enhanced covariant strains are pushed forward to those in the physical coordinates. It is important to notice here that the matrix $\mathbf{M}(\boldsymbol{\xi})$ needs to satisfy the following condition [8]:

$$\int \mathbf{M}(\boldsymbol{\xi})d\boldsymbol{\xi} = \mathbf{0} \tag{19}$$

such that the following orthogonality condition of the assumed stress and strain is satisfied:

$$\int_{V_0} \boldsymbol{\sigma}\cdot\boldsymbol{\varepsilon}^{EAS} dV_0 = 0 \tag{20}$$

Using the preceding condition, the assumed stress term that appears in Hu-Washizu mixed variational principle vanishes and one can obtain the generalized elastic force vector as follows [8]:

$$\mathbf{Q}_k = \int_{V_0}\left(\frac{\partial \boldsymbol{\varepsilon}^c}{\partial \mathbf{e}}\right)^T \frac{\partial W(\boldsymbol{\varepsilon}^c + \boldsymbol{\varepsilon}^{EAS})}{\partial \boldsymbol{\varepsilon}} dV_0 \tag{21}$$

where W is an elastic energy function. Furthermore, the internal EAS parameters are determined by solving the following equations for each element i:

$$\int_{V_0^i}\left(\frac{\partial \boldsymbol{\varepsilon}^{EAS}}{\partial \boldsymbol{\alpha}^i}\right)^T (\boldsymbol{\varepsilon}^c + \boldsymbol{\varepsilon}^{EAS})\, dV_0^i = \mathbf{0} \tag{22}$$

3.3 Thickness Locking

In addition to locking problems associated with the shear and in-plane strains discussed in the previous subsection, the element locking associated with the transverse normal strain is exhibited in the bi-linear ANCF shell element due to the use of the transverse gradient coordinates, and the thickness locking has a significant impact on the accuracy of this type of element. The solid shell elements which consists of layers of translational nodal coordinates at the top and bottom surfaces of the element [15-17] and shell elements parameterized by extensible directors [12-14] also suffer from the thickness locking resulting from the erroneous transverse normal strain distribution. The use of the assumed natural strain (ANS) approach is proposed in the literature [12] for the shell element with extensible directors and the transverse normal strain at a material point in the element is assumed as follows:

$$\varepsilon_{zz}^{ANS} = S_1^{ANS}\varepsilon_{zz}^1 + S_2^{ANS}\varepsilon_{zz}^2 + S_3^{ANS}\varepsilon_{zz}^3 + S_4^{ANS}\varepsilon_{zz}^4 \tag{23}$$

where ε_{zz}^k indicates the compatible transverse strain at node k and S_k^{ANS} indicates the shape function associated with it. It is shown in the literature [7] that use of this approach eliminate the thickness locking of the bi-linear shear deformable ANCF flat plate element formulated by the elastic plane approach, in which the strain distribution along the thickness is assumed to be constant.

Another approach is the use of the enhanced assumed strain (EAS) approach [8]. In this case, additional internal EAS parameters $\boldsymbol{\alpha}$ are introduced to enhance the transverse normal strain field. In the continuum mechanics approach, the elastic forces of the shell element is formulated as a continuum volume, thus the strain distribution along the thickness is not assumed to be constant unlike the elastic plane approach. This leads to severe thickness locking exhibited in the continuum mechanics

based ANCF shell element. For this reason, the transverse strain modified by the assumed natural strain approach is further modified as follows:

$$\varepsilon_{zz} = \varepsilon_{zz}^{ANS} + \varepsilon_{zz}^{EAS} \tag{24}$$

In the preceding equations introduced in this investigation for the bi-linear shear deformable ANCF shell element, the compatible strain ε_{zz}^{c} is replaced with the assumed natural strain given by Eq. 23. Since it is not guaranteed that transverse strains at nodal points (sampling points) are always accurate in Eq. 23, the assumed strain field is further enhanced by the enhanced assumed strain approach. In the combined ANS and EAS approach for the transverse normal strain applied to the continuum mechanics based ANCF shell element, the covariant strain components of the transverse shear and transverse normal strains are interpolated in the natural coordinate system and the covariant strain vector given in Eq. 12 is replaced with the following strain vector:

$$\tilde{\boldsymbol{\varepsilon}} = \left[\tilde{\varepsilon}_{xx} \quad \tilde{\varepsilon}_{yy} \quad \tilde{\varepsilon}_{zz}^{ANS} \quad \tilde{\gamma}_{xy} \quad \tilde{\gamma}_{xz}^{ANS} \quad \tilde{\gamma}_{yz}^{ANS} \right]^T \tag{25}$$

and then the Green-Lagrange strains are evaluated using the transformation defined by Eq. 11 and the enhanced assumed strains associated with ε_{xx}^{EAS} , ε_{yy}^{EAS} , γ_{xy}^{EAS} and ε_{zz}^{EAS} are added. This leads to a systematic derivation of the generalized elastic forces for the locking-free continuum mechanics based shear deformable ANCF shell element.

4. NUMERICAL EXAMPLES

In this section, several numerical examples are presented in order to demonstrate the performance of the continuum mechanics based bi-linear shear deformable ANCF shell element developed in this investigation. The effect of the assumed natural strain and enhanced assumed strain approaches on the element accuracy is also discussed.

4.1 Cantilevered Plate and Shell Subjected to a Point Force

In the first problem, a rectangular cantilevered plate subjected to a vertical point force at one of the corner of the plate is considered as shown in Fig. 3. The length, width, and thickness of the plate are assumed to be $\ell = 1.0$ m, $w = 1.0$ m, and $h = 0.01$ m. The Young's modulus and Poisson's ratio are assumed to be $E = 2.1 \times 10^8$ Pa and $\nu = 0.3$, respectively. As shown in Fig. 3, the plate is subjected to large deformation at the static equilibrium state. The six models with different strain modifications discussed in Section 3 are considered to demonstrate the effect of the EAS and ANS approaches on the element accuracy. These models are summarized in Table 1. In Model-1, any strain modifications are not made, while Model-6 has the combined ANS and EAS approach for the thickness locking together with ANS for the transverse shear and EAS for the in-plane normal and shear.

The error of the vertical deflection at the corner of the plate edge is presented as a function of the number of elements in Fig. 4. The numerical error is defined by difference from the reference solution obtained using ANSYS SHELL181 with 100×100 elements. The results obtained by ANSYS SHELL181 and the bi-linear shear deformable ANCF flat plate element using the elastic plane approach [7] are also presented for comparison. It is observed from this figure that use of Model-6 with the combined ANS and EAS approach leads to the identical result with that of the locking-free ANCF flat plate element using the elastic plane approach. It is important to notice here that the plate element obtained using the elastic plane approach employs ANS for alleviating the thickness locking, while Model-4 of the continuum mechanics approach that uses the same strain modification does not eliminate the thickness locking completely. While the application of EAS to the thickness locking improves the element performance as shown in the result of Model-5, the accuracy is not satisfactory especially when the small number of elements is used. This result clearly indicates severity of the thickness locking exhibited in the continuum mechanics based ANCF shell element and the thickness locking of the shell element, in which the elastic forces are formulated as a continuum volume, needs to be eliminated using the combined EAS and ANS approach as discussed in Section 3. The effect of ANS for the transverse shear locking is shown by the comparison between Model-1 and Model-2, while the effect of EAS for the in-plane normal and shear locking is shown by the comparison between Model-3 and Model-4, with which it is shown that the in-plane normal and shear locking effect is not significant in this problem.

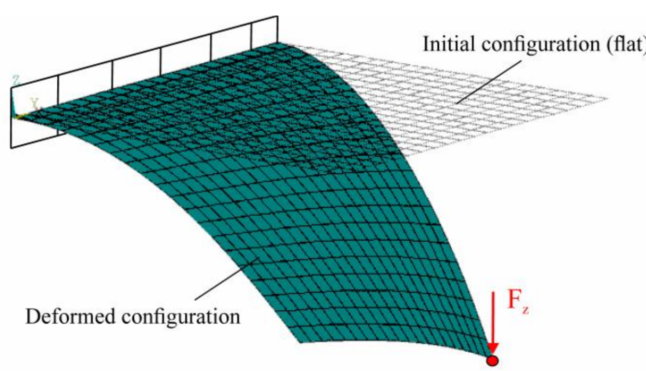

Figure 3. Deformed shape of a cantilevered plate subjected to a large transverse tip load

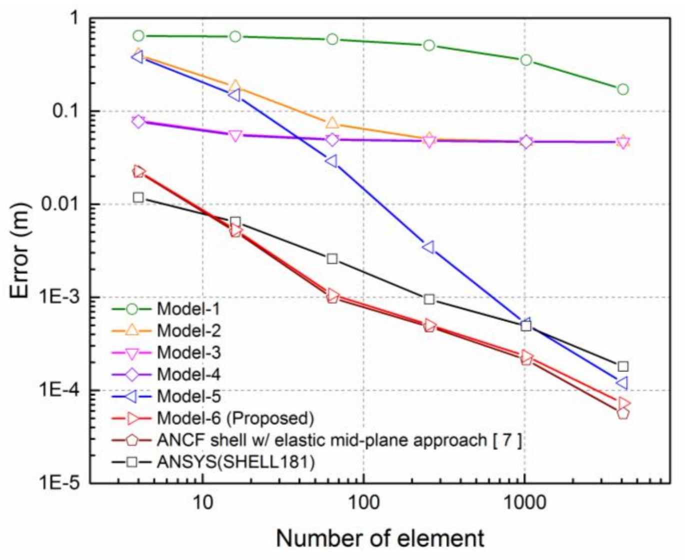

Figure 4. Numerical convergence with large deformation (initially flat)

In the second problem, the flat plate is replaced with the quarter cylinder modeled by the continuum mechanics based bi-linear ANCF shell elements as shown in Fig. 5 while keeping the same material properties, tip load, width and height. The radius of curvature is assumed to be 1.0 m. The deformed shape in static equilibrium is shown in Fig. 5 and the large deformation is exhibited in this problem. The error of the numerical solutions is presented in Fig. 6 for Models 1 to 6 and ANSYS SHELL181. The trend of the convergence rate and the accuracy is similar to that observed for the flat plate problem, and the use of the combine EAS and ANS approach leads to the suitable rate of convergence and accuracy for shell structures.

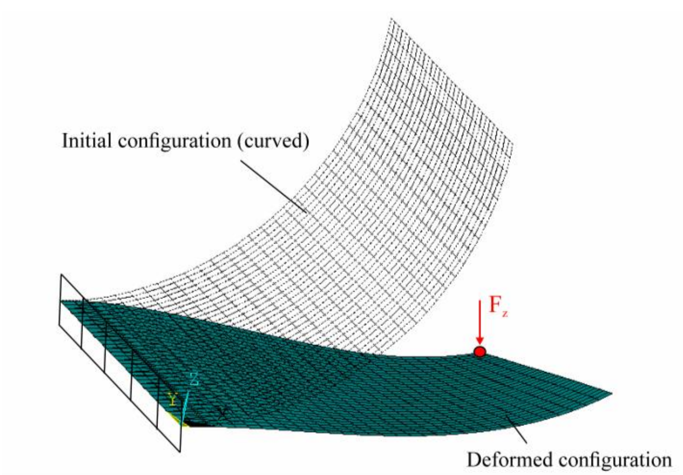

Figure 5. Deformed shape of a cantilevered shell subjected to a large transverse tip load (initially curved)

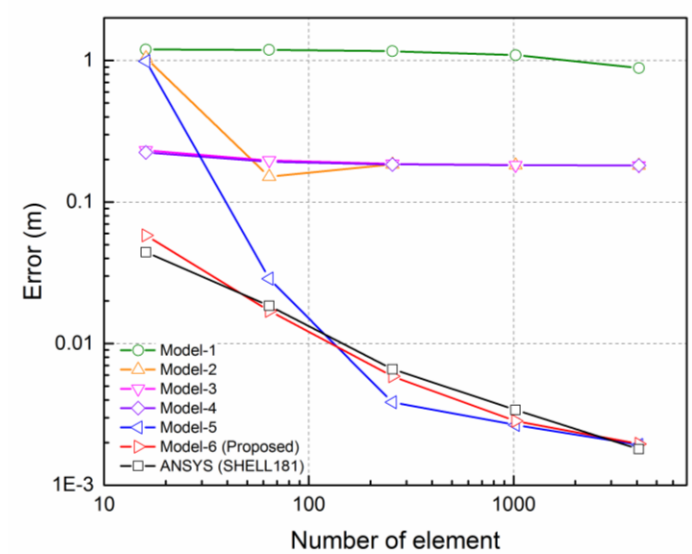

Figure 6. Numerical convergence with large deformation (initially curved)

4.2 Quarter Cylinder Pendulum

In the third problem, the quarter cylinder that has the same dimension as the one discussed in the previous subsection is used for the nonlinear dynamics problem. A corner of the plate is connected to ground by spherical joint as shown in Fig. 7 and the deformed shapes of the quarter cylinder under the effect of gravity are shown in Fig. 7. In this problem, Young's modulus is reduced to $E = 2.1\times10^7$ Pa to demonstrate the motion with large deformation. The global position at point A shown in Fig. 7 is presented in Fig. 8 for different number of elements, and the results are compared with those obtained using the cubic ANCF thin shell element [19] with 20×20 elements. While the effect of the shear deformation is not noticeable in the gross motion of the quarter cylinder, the numerical result is in good agreement with those of the continuum mechanics shear deformable ANCF shell element developed in this investigation.

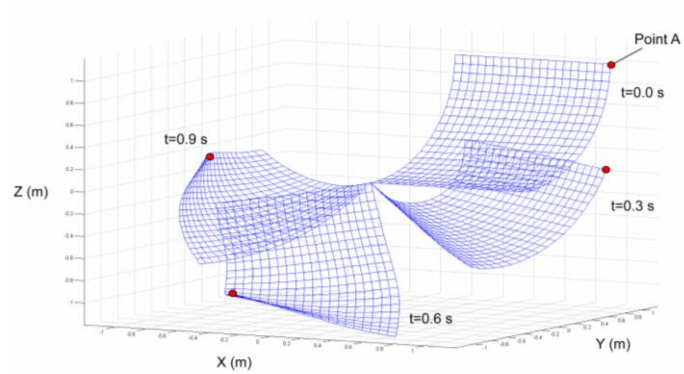

Figure 7. Deformed configuration of nonlinear dynamics (initially curved shell element)

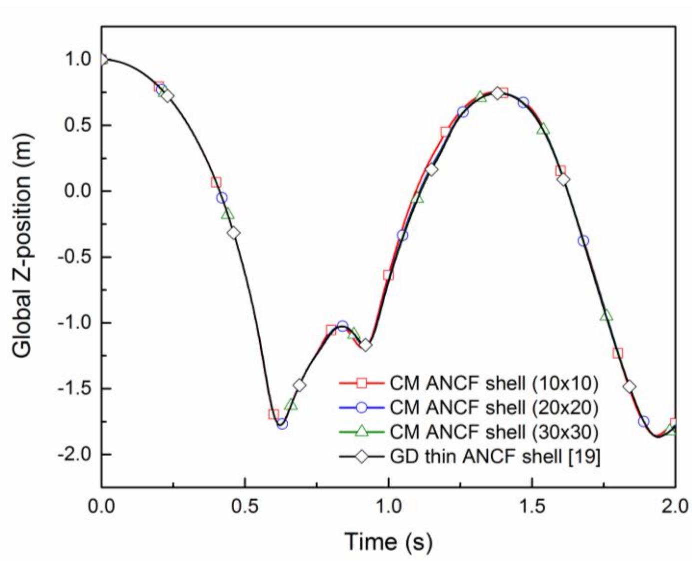

Figure 8. Global Z-position at Point A with bi-linear ANCF shell element

the continuum mechanics based bi-linear shear deformable ANCF shell element can be eliminated. The shear locking as well as the in-plane normal and shear locking are also eliminated using the assumed natural strain and the enhanced assumed strain approaches, respectively, in a standard manner. The locking-free shear deformable element developed in this investigation can be used for modeling a wide variety of large deformable multibody shell structures with material nonlinearities that include pneumatic tires in vehicle dynamics simulation as well as rotor blades in the wind turbine dynamics simulation.

ACKNOWLEDGEMENTS

The authors wish to acknowledge the financial support of the Automotive Research Center (ARC) in accordance with Cooperative Agreement W56HZV-04-2-0001 U.S. Army Tank Automotive Research, Development and Engineering Center (TARDEC). Financial support for the last author received from FunctionBay Inc is acknowledged.

Table 1. Strain modification for the continuum mechanics based ANCF bi-linear shell element

Model name	ANS for transverse shear strains $\varepsilon_{xz/yz}^{\mathrm{ANS}}$	EAS for in-plane strains $\varepsilon_{xx/yy/xy}^{\mathrm{EAS}}$	ANS for transverse normal strain $\varepsilon_{zz}^{\mathrm{ANS}}$	EAS for transverse normal strain $\varepsilon_{zz}^{\mathrm{EAS}}$	Combined EAS and EAS for transverse normal strain $\varepsilon_{zz}^{\mathrm{ANS/EAS}}$
Model-1	-	-	-	-	-
Model-2	Y	-	-	-	-
Model-3	Y	-	Y	-	-
Model-4	Y	Y	Y	-	-
Model-5	Y	Y	-	Y	-
Model-6	Y	Y	-	-	Y

5. SUMMARY AND CONCLUSIONS

In this investigation, a bi-linear shear deformable shell element is developed using the absolute nodal coordinate formulation for the large deformation analysis of multibody shell structures. The elastic forces are formulated using the continuum mechanics approach which allows for the consideration of nonlinear material model such as hyperelasticity in the shell element in a straight forward manner. It is demonstrated that the use of the continuum mechanics approach leads to severe thickness locking which needs to be carefully handled in the element formulation. To overcome the difficulty associated with the thickness locking of the element, the transverse normal strain modified by the assumed natural strain approach is further enhanced by the enhanced assumed strain approach. It is demonstrated by several numerical examples that the combined ANS and EAS approach leads to the better approximation of the transverse normal strain, and the thickness locking exhibited in

REFERENCES

[1] Mikkola, A. M., and Shabana, A. A., 2003, “A Non-Incremental Finite Element Procedure for The Analysis of Large Deformation of Plates and Shells in Mechanical System Applications”, *Multibody System Dynamics*, Vol. 9, pp.283-309.

[2] Dufva, K., and Shabana, A. A., 2005, “Analysis of Thin Plate Structures Using The Absolute Nodal Coordinate Formulation”, *Proceedings of the Institution of Mechanical Engineers, Part K: Journal of Multi-body Dynamics*, Vol. 219, pp. 345-355.

[3] Schwab, A. L., Gerstmayr, J., and Meijaard, J. P., 2007, “Comparison of Three-Dimensional Flexible Thin Plate Elements for Multibody Dynamic Analysis: Finite Element Formulation and Absolute Nodal Coordinate Formulation”, *Proceedings of the ASME 2007*

International Design Engineering Technical Conferences & Computers and Information in Engineering Conference, Las Vegas, Nevada, USA.

[4] Matikainen, M.K., Valkeapää, A. I., Mikkola, A. M., and Schwab, A. L., 2013, "A Study of Moderately Thick Quadrilateral Plate Elements Based on the Absolute Nodal Coordinate Formulation", *Multibody System Dynamics*, pp. 1–30.

[5] Dmitrochenko, O., Matikainen, M., and Mikkola, A., 2012, "The Simplest 3- and 4-Noded Fully Parameterized ANCF Plate Elements", *Proceedings of the ASME 2012 International Design Engineering Technical Conferences & Computers and Information in Engineering Conference*, Chicago, IL, USA

[6] Nachbagauer, K., Gruber, P., and Gerstmayr, J., 2013, "Structural and Continuum Mechanics Approaches for a 3D Shear Deformable ANCF Beam Finite Element: Application to Static and Linearized Dynamic Examples", *ASME Journal of Computational and Nonlinear Dyanamics*, Vol. 8, pp.021004-1-7

[7] Valkeapää, A. I., Yamashita, H., Jayakumar, P. and Sugiyama, H., "Gradient Deficient Bi-Linear Plate Element Based on Absolute Nodal Coordinate Formulation", in preparation.

[8] Simo, J. C., and Rifai, M. S., 1990, "A Class of Mixed Assummed Strain Methods and The Method of Incompatible Modes", *International Journal for Numerical Methods in Engineering*, Vol. 29, pp.1595-1638.

[9] Andelfinger, U., and Ramm, E., 1993, "EAS-Elements for Two-Dimensional, Three-Dimensional, Plate and Shell Structures and Their Equivalence to HR-Elements", *International Journal for Numerical Methods in Engineering*, Vol. 36, pp.1311-1337.

[10] Dvorkin, E. N., and Bathe, K. J., 1984, "A Continuum Mechanics Based Four-Node Shell Element for General Non-Linear Analysis", *Engineering Computations*, Vol. 1, pp.77-88.

[11] Bathe, K. J. and Dvorkin, E. N., 1986, "A Formulation of General Shell Elements - The Use of Mixed Interpolation of Tensorial Components", *International Journal for Numerical Methods in Engineering*, Vol. 22, pp.697-722.

[12] Betsch, P., and Stein, E., 1995, "An Assumed Strain Approach Avoiding Artificial Thickness Straining for A Non-Linear 4-Node Shell Element", *Communications in Numerical Methods in Engineering*, Vol. 11, pp. 899-909.

[13] Betsch, P., Gruttmann, F., and Stein, E., 1996, "A 4-Node Finite Shell Element for the Implementation of General Hyperelastic 3D-Elasticity at Finite Strains", *Computer Methods in Applied Mechanics and Engineering*, Vol. 130, pp. 57-79.

[14] Bischoff, M., Ramm, E., 1997, "Shear Deformable Shell Elements for Large Strains and Rotations", *International Journal for Numerical Methods in Engineering*, Vol. 40, pp.4427-4449.

[15] Hauptmann, R., and Schweizerhof, K., 1998, "A Systematic Development of 'Solid-Shell' Element Formulations for Linear and Non-Linear Analyses Employing Only Displacement Degrees of Freedom", *International Journal for Numerical Methods in Engineering*, Vol. 42, pp.49-69.

[16] Vu-Quoc, L., and Tan, X. G., 2003, "Optimal Solid Shells for Non-Linear Analyses of Multilayer Composites. Ⅰ. Statics", *Computer Methods in Applied Mechanics and Engineering*, Vol. 192, pp. 975-1016.

[17] Mostafa, M., Sivaselvan, M. V. and Felippa, C. A., 2013, "A Solid-Shell Corotational Element Based on ANDES, ANS and EAS for Geometrically Nonlinear Structural Analysis", *International Journal for Numerical Methods in Engineering*, Vol. 95, pp.145-180.

[18] Cook, R. D., Malkus, D. S., Plesha, M. E., and Witt, R. J., 2002, *Concepts and Applications of Finite Element Analysis Fourth Edition*, Wiley.

[19] Yan, D., Liu, C., Tian, Q. et al, 2013, "A New Curved Gradient Deficient Shell Element of Absolute Nodal Coordinate Formulation for Modeling Thin Shell Structures", *Nonlinear Dynamics*, Vol.74, pp.153-164.

